Advanced Journal of Chemistry, Section A

Journal homepage: www.ajchem-a.com

Original Research Article

Synthesis of Chitosan Films Incorporated with *Andrographis paniculata* (Burm. F.) Nees Extract by Supercritical CO_2 Technique and Their Biological Activities

Le Ngoc Quynh Chau[1,2,3], Pham Trong Liem Chau[1,2,3], Tran Nguyen Cam Nhung[1,2,3], Huynh Ngoc Oanh[1,2,3], Le Xuan Tien[1,2,3], Nguyen Huu Hieu[1,2,3,*]

[1]*VNU-HCM, Key Laboratory of Chemical Engineering and Petroleum Processing (Key CEPP Lab), Ho Chi Minh City University of Technology (HCMUT), 268 Ly Thuong Kiet Street, Dien Hong Ward, Ho Chi Minh City, Vietnam*
[2]*Faculty of Chemical Engineering, Ho Chi Minh City University of Technology (HCMUT), 268 Ly Thuong Kiet Street, Dien Hong Ward, Ho Chi Minh City, Vietnam*
[3]*Vietnam National University Ho Chi Minh City, Linh Xuan Ward,Ho Chi Minh City, Vietnam*

ARTICLEINFO

Article history

Submitted: 2026-01-02
Revised: 2026-02-03
Accepted: 2026-02-21
ID: AJCA-2601-2035
DOI: 10.48309/AJCS.2026.572011.2035

KEYWORDS

Andrographis paniculata
Supercritical CO_2
Chitosan
Biological activities

ABSTRACT

In this study, *Andrographis paniculata* (Burm. F.) Nees extract was obtained using the supercritical carbon dioxide (CO_2) extraction method, a green and sustainable alternative to conventional solvent-based techniques. Chitosan (CTS) films, both with and without the *A. paniculata* extract (APE), were prepared using the solution-casting method. The effects of varying APE levels (1, 2, and 3 mL) incorporated into the CTS solution on the films' physical properties, such as color, light transmittance, moisture content, water solubility, and water vapor permeability, were systematically studied. The mechanical properties, including moisture content, swelling degree, and solubility, were also evaluated. Characterization of the synthesized films was conducted using advanced analytical techniques, including Fourier-transform infrared spectroscopy (FTIR), UV-visible absorption spectroscopy, scanning electron microscopy (SEM), and energy-dispersive X-ray spectroscopy (EDS). Additionally, the biological properties of the films were assessed, focusing on their antibacterial activity against Gram-positive *Staphylococcus aureus* and Gram-negative *Pseudomonas aeruginosa*, as well as their anti-inflammatory activity. Results revealed that CTS-2APE and CTS-3APE films exhibited significantly enhanced antibacterial activity compared to CTS alone, as evidenced by larger inhibition zones. Furthermore, the films containing APE demonstrated superior anti-inflammatory activity against egg albumin denaturation across various concentrations. These findings indicate that the incorporation of APE into CTS films enhances both their antibacterial and anti-inflammatory properties, making them promising candidates for biological activities.

* Corresponding author: Nguyen Huu Hieu
✉ E-mail: nhhieubk@hcmut.edu.vn

GRAPHICAL ABSTRACT

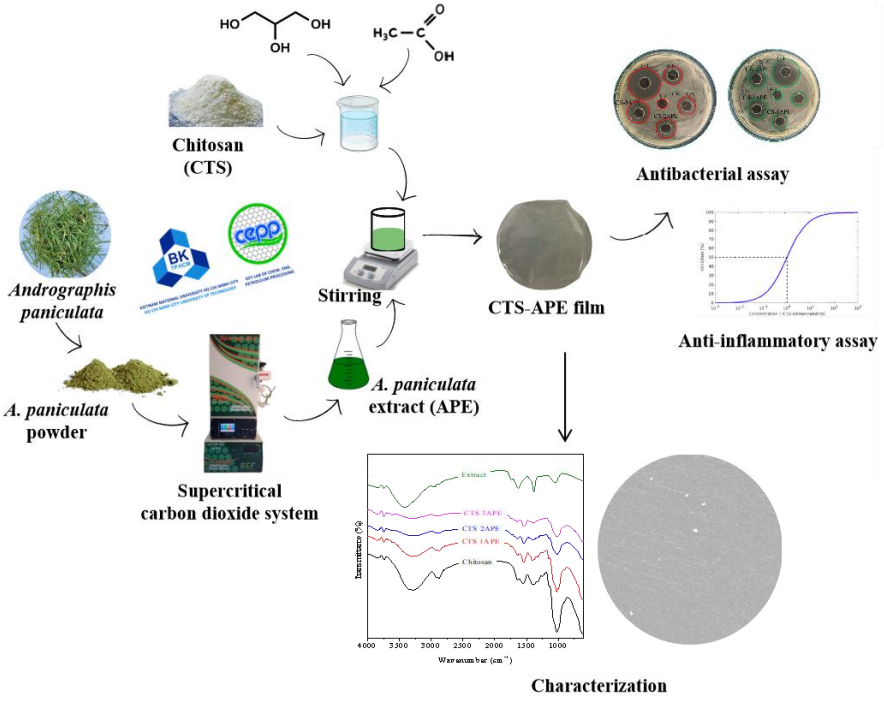

Introduction

In recent years, medical waste has significantly increased globally due to several interconnected factors. The rising demand for healthcare services, driven by population growth, aging demographics, and escalating chronic diseases, necessitates more frequent medical interventions and treatments, thereby generating greater amounts of waste [1]. As the population ages and chronic diseases such as diabetes, cardiovascular diseases, and cancer become more prevalent, many individuals concurrently suffer from multiple chronic conditions, leading to increased medical consultations, tests, and treatments that contribute significantly to waste generation. Modern medical advancements, including complex procedures and the widespread use of disposable devices and materials, also contribute to this trend. Additionally, a cultural shift towards single-use items in healthcare settings, motivated by infection control measures and operational efficiencies, exacerbates the accumulation of medical waste [2]. Recent global health crises, such as the COVID-19 pandemic, have further intensified this issue with heightened healthcare activities and extensive use of single-use personal protective equipment. Statistically, approximately 240 tons of healthcare waste per day were generated in Wuhan during the peak of the pandemic, which is about six times higher than before the pandemic occurred [3]. The escalating volume of medical waste poses significant environmental risks if left unchecked. Improper disposal of medical waste, which typically contains heavy metals and synthetic chemicals, can lead to the spread of toxic substances in the environment, resulting in land and water pollution that poses threats to human health. Furthermore, the appearance of drug-resistant microorganisms from medical facilities into the environment poses a potential contagion risk. The accumulation of non-biodegradable materials such as plastics from single-use medical items also contributes to marine debris and landfills, further

exacerbating environmental pollution and ecosystem degradation [4]. Therefore, sustainable management practices, including waste reduction and adherence to stringent disposal regulations, are crucial in mitigating these environmental impacts and safeguarding ecological balance and human well-being in the face of mounting medical waste volumes.

Over the last few decades, research has been conducted to find and innovate materials as alternatives to petroleum-based plastics used in the medical field. This effort aims to reduce the noticeable increase in healthcare waste volume. Certain materials, such as polylactic acid, chitosan (CTS), cellulose derivatives, silk fibroin, and alginate, have been found to offer promising solutions to reduce reliance on petroleum-based plastics in the medical field [5]. These materials address environmental concerns and promote sustainable healthcare practices due to their biocompatibility and biodegradability. Among these biopolymers, CTS offers several advantages, including antimicrobial effects, anticoagulant properties, wound healing capabilities, versatility, and being a renewable source [6]. This natural polymer is also considered relatively non-toxic to animals and well-tolerated by the human body. Furthermore, CTS is proven to be the only polycation existing in nature, with its charge density controlled by the pH of the medium and the degree of acetylation [7]. It is also reported to be utilized in various biomedical applications, including wound healing accelerators, artificial kidney films, carriers for controlled release in drug delivery systems, and artificial skin due to its beneficial properties [8]. Meanwhile, extracts from medicinal plants and their incorporation into CTS-based films have been explored as promising approaches in biomedical applications to enhance biological properties and modify certain physical properties due to the effective phytochemical compounds present in the extract. *Andrographis paniculata* (*A. paniculata*), characterized by its green color, aromatic smell, and bitter taste, is an herbaceous plant found throughout tropical, subtropical Asia, Southeast Asia, and India [9]. It holds significant importance as a medicinal herb and is widely used around the world, particularly in many Asian countries, as a traditional herbal medicine. A notable number of bioactive compounds, including flavonoids, diterpenoids, and polyphenols, have been isolated from various parts of *A. paniculata* such as leaves, stems, and roots. These chemical compounds are assumed to be the major factors responsible for the pharmacological effects of *A. paniculata*, with andrographolide, an active diterpenoid, identified as the predominant compound due to its relatively high concentration [10]. According to various pharmacological investigations, *A. paniculata* extract (APE) exhibits a variety of biological activities, including antibacterial, antiviral, antidiabetic, anticancer, hemolytic, and hepatoprotective effects [11]. However, active chemical constituents in the plant extract are easily destroyed, obtained in low yield, and often require substantial amounts of organic solvents, which are known for their typical toxicity, during extraction processes if conventional extraction methods such as Soxhlet extraction, heat-assisted extraction, and vacuum extraction are employed. To avoid these issues, modern technology utilizing supercritical CO_2 as the main solvent is employed for the extraction of natural compounds since carbon dioxide is easily accessible with high purity, at a low cost, and possesses non-combustible, non-toxic properties. Furthermore, supercritical CO_2 exhibits accelerated extraction due to the faster mass transfer facilitated by the higher diffusivity and lower viscosity of carbon dioxide. As a result, employing supercritical CO_2 for the extraction of *A. paniculata* helps to preserve the beneficial properties of the medicinal plant when combined with CTS to synthesize biodegradable films with biological activities.

Therefore, this present study aims to synthesize chitosan (CS) films incorporated with APE, which

is obtained through the supercritical CO_2 extraction technique. The effect of APE addition (1, 2, and 3 mL) combined with the CTS solution on the physical properties, mechanical properties, and characterization of the films was investigated, using techniques such as Fourier-transform infrared spectroscopy (FTIR), UV-visible absorption spectroscopy (UV-Vis), scanning electron microscopy (SEM), and energy-dispersive X-ray spectroscopy (EDX). Additionally, antibacterial and anti-inflammatory activities were evaluated using the Kirby-Bauer well diffusion method and the egg albumin denaturation assay.

Experimental

Materials and chemicals

Dried *A. paniculata* leaves were purchased from Tan Phat Company, Ho Chi Minh City, Vietnam. CTS powder was obtained from S-GREEN Investment Joint Stock, District 8, Ho Chi Minh City. Acetic acid, ethanol, glycerol, potassium bromide, potassium chloride, sodium chloride, monopotassium phosphate, and disodium phosphate were supplied by Xilong Scientific, China. All chemicals were used as received, without further purification.

The bacterial strains of *Staphylococcus aureus* (*S. aureus*) ATCC® 25923™ and *Pseudomonas aeruginosa* (*P. aeruginosa*) ATCC® 25922™ used in the experiments were obtained from the Pasteur Institute in Ho Chi Minh City, Vietnam. Furthermore, sheep blood agar medium and buffer were procured from Nam Khoa Biotek Co., Vietnam.

Preparation of Andrographis paniculata extract

The dried *A. paniculata* leaves were ground into powder before being processed through the supercritical CO_2 system. The powder underwent extraction using supercritical CO_2 as the main solvent in a supercritical CO_2 extraction machine operating at 60 °C and 350 bar for 2 hours. Subsequently, the extract from the dried *A. paniculata* was obtained for further use.

Preparation of the films

CTS films combined with APE were fabricated using the solution-casting method [12,13]. Initially, CTS powder was dissolved in a 1 wt% acetic acid solution to prepare the CTS solution. Subsequently, specific amounts of APE (1, 2, and 3 mL) were added to 30 mL of CTS solution to create CS-1APE, CS-2APE, and CS-3APE, respectively, resulting in four blended films. The mixture was then stirred using a magnetic stirrer for one hour to obtain a transparent solution. Glycerol was subsequently added to this solution and mixed using a magnetic stirrer. After an additional hour of stirring, the solution was poured into a petri dish and spread evenly. Finally, after drying at 40 °C, the CTS films incorporated with the extract were achieved.

Physical properties of the films

Colour appearance and transmittance

The transmittance of CTS and CTS-xAPE (x = 1, 2, and 3) films supplemented with extract was measured from 200 to 800 nm using the Genesys 50 UV-Vis Spectrophotometer from Thermo Fisher Scientific, USA.

Moisture content, swelling degree, and solubility

The moisture content, swelling degree, and solubility of the fabricated films were determined according to a previous study [14]. The synthesized films were cut into 2 × 2 cm pieces, and their initial weights (m_1) were measured using an analytical balance with a readability of 0.1 mg. The samples were then dried at 70 °C for 24 hours, and the weights of the dried films were recorded as m_2. Next, these film samples were immersed in a pH 7.0 solution at room

temperature for 24 hours. After immersion, excess water not absorbed by the films was gently removed using filter paper, and the films were weighed to obtain data for m_3. The films were dried again at 70 °C for 24 hours to obtain their final weights (m_4). The moisture content, swelling degree, and solubility were calculated using Equations 1-3.

$$\text{Moisture content (\%)} = \frac{m_1 - m_2}{m_1} \times 100\% \quad (1)$$

$$\text{Swelling degree (\%)} = \frac{m_3 - m_2}{m_2} \times 100\% \quad (2)$$

$$\text{Solubility (\%)} = \frac{m_2 - m_4}{m_2} \times 100\% \quad (3)$$

Mechanical properties

The thickness, tensile strength, and elongation at break of the films were examined. The fabricated films (1 × 8 cm) were tested using a texture analyzer (AG-Xplus Series Precision Universal Testers). Each film was measured at least three times, and the average data were collected.

Characterization of the films

FTIR spectroscopy of the synthesized films and the extract was conducted using an Alpha–E FTIR spectrometer from Bruker Optik GmbH, Ettlingen, Germany, equipped with an attenuated total reflection (ATR) accessory.

The morphological and elemental analyses of the samples were conducted using SEM images and EDX spectra captured with a JSM-IT 200 from JEOL, Japan. Measurements were performed at an acceleration voltage of 10 kV, with a magnification of ×1000 and a resolution of 512 × 384 pixels.

Antimicrobial activity

The antibacterial activity of the CTS films incorporated with APE was investigated against two bacterial strains, *P. aeruginosa* and *S. aureus*, using the Kirby-Bauer well diffusion method [15]. Luria-Bertani agar (LBA) was used as the culture medium to provide nutrients and specific minerals for bacterial growth and maintenance during the antibacterial test. Additionally, gentamicin, an aminoglycoside and bactericidal antibiotic, served as a positive control in this assay. Bacterial suspensions of *S. aureus* and *P. aeruginosa* were prepared for the well diffusion method. A sterile swab was dipped into the bacterial suspension to collect the bacteria and transfer the inoculum onto the agar plates. The samples were then applied to the wells on the agar. After 24 hours of incubation, clear zones known as zones of inhibition were observed. The diameters of these zones were measured and compared to analyze the antibacterial effects.

Anti-inflammatory

To determine the *in vitro* anti-inflammatory properties of the synthesized films, an egg albumin denaturation assay was performed. A fixed amount of sample solution, distilled water, phosphate-buffered saline, and a 1% albumin solution were transferred to test tubes. The test tubes were left at room temperature for 30 minutes and then placed in a 70 °C oven for 15 minutes to accelerate protein denaturation. After 15 minutes, the test tubes were cooled to room temperature and analyzed using a UV-Vis spectrometer to determine the absorbance. The percentage inhibition of the synthesized films was then computed from the absorbance data for evaluation, using Equation 4.

$$\text{\% Inhibition} = \frac{ODc - (ODt - ODcs)}{ODc} \times 100\% \quad (4)$$

Where, ODc is the optical density of test control solution, ODt is the optical density of test solution, and ODcs is the optical density of product control solution.

Results and Discussion

Physical properties of the films

The appearance and color of the synthesized films are pivotal factors to consider. In this study,

the colors of the fabricated films varied noticeably with different quantities of the extract added. Distinct color differences were observed between the control film and the films incorporated with APE. Hues such as green, yellow, and brown were noted in varying degrees in the films with added extract. Specifically, the color of the films tended to darken with increasing amounts of extract. For instance, the CTS film with the highest amount of extract (3 mL) exhibited the darkest color compared to the others. In contrast, the control film without extract was colorless and transparent. The color changes observed in the CTS-based films with added plant extract, compared to the control film, align with findings reported in previous studies [5]. The color in the CTS-based films when the extract is added can be attributed to the presence of plant pigments [6]. Additionally, the brownish hue observed in the films may result from the oxidation of polyphenols during the drying and storage stages of the film synthesis process [16]. Visually, the surface of the films was relatively smooth, with no visible cracks or wrinkles. No discernible bubbles or irregular pores were detected with the naked eye. Although the films darkened with increasing extract amounts, their transparency was not significantly reduced, as the Petri dishes remained visible through the CTS-based films.

Light transmission is a crucial factor when selecting materials for wound dressings, as ultraviolet (UV) radiation can influence and delay the wound-healing process in various ways [17]. Specifically, ultraviolet A radiation is reported to delay wound contraction and decrease collagen content in healing wounds [18]. Figure 1 illustrates the transmittance of the synthesized films across UV and visible wavelengths. Generally, the CTS sample exhibited the highest percentage of transmittance to both UV and visible light compared to the other samples, meaning it had the lowest ability to inhibit light transmission. The introduction of APE into the CTS-based films significantly reduced transmittance across various degrees. In the UV wavelength range of 200-400 nm, which includes UV radiation, the films blended with extract showed notably lower transmittance compared to the control film. Specifically, in the UV-C range (200-280 nm), the difference in light inhibition performance was most apparent. While the CTS sample had approximately 50% transmittance in

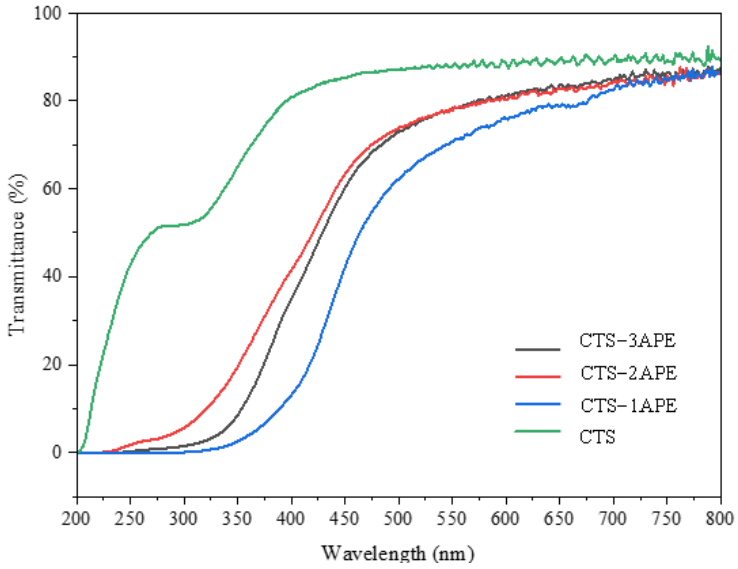

Figure 1. Transmittance of the synthesized films

the UV-C wavelength, the CTS-xAPE samples showed nearly 0% transmittance. In the UV-B range (280-320 nm), the transmittance was relatively low, with a maximum value of approximately 10%, indicating effective UV-B absorption by the films. Similarly, the transmittance in the UV-A range (320-400 nm) and visible light (400-700 nm) was significantly lower in the CTS-xAPE films compared to the CTS film. Based on the transmittance results, the CTS-3APE film is the most effective in UV protection among all the films surveyed. In other words, the CTS-3APE film can prevent almost all UV transmission in the 200-350 nm wavelength range. Conversely, the CTS film has the lowest efficacy in UV protection. The decrease in transmittance values indicates the ability of the films incorporated with APE to absorb UV radiation and provide a temporary protective physical barrier. This phenomenon can be explained by the presence of aromatic compounds in the extract, which have strong UV-Vis light absorption properties, and the hydrogen bonding between polyphenol compounds and the CTS matrix [19,20]. The reduction in transmittance of CTS-based films with added extract has also been observed and documented in previous studies.

Mechanical properties of the films

Thickness

Thickness, mechanical resistance, and flexibility are fundamental characteristics of films, and these parameters were examined to evaluate and understand the behaviors of the synthesized films. Specifically, mechanical resistance and flexibility are typically assessed through tensile strength and elongation at break, respectively. Tensile strength is defined as the maximum load stress that materials can withstand during a tension test. Table 1 presents the thickness, tensile strength, and elongation at break of the fabricated films. The incorporation of APE did not significantly change the thickness of the films. However, the addition of the extract noticeably affected the mechanical properties, as evidenced by the differences in tensile strength and elongation at break among the films. The tensile strength and elongation at break of the CTS film were recorded at 39.63 ± 7.39 MPa and 96.34 ± 27.75%, respectively. These values are relatively higher compared to those reported for glycerol-plasticized CTS films, which were 26.86 ± 3.50 MPa and 3.72 ± 0.57%, respectively [6]. Differences may arise due to factors such as molecular weight, degree of deacetylation, analytical methods, film fabrication techniques, and storage conditions. The introduction of APE in smaller amounts led to a decrease in tensile strength and elongation at break. For instance, the CTS-1APE film had tensile strength and elongation at break values of 37.45 ± 17.08 MPa and 93.74 ± 24.71%, respectively. Similarly, the CTS-3APE film showed a reduction in elongation at break to 95.88 ± 19.97%. These reductions can be attributed to the partial replacement of stronger polymer-polymer interactions with weaker hydrogen bonds between the polymer and the extract compounds, leading to increased interchain distances and reduced intermolecular forces [10,21]. Conversely, increases in tensile strength were observed in the CTS-2APE and CTS-3APE films compared to the CTS film. Specifically, the CTS-2APE film exhibited the highest tensile strength at 51.72 ± 12.77 MPa, followed by the CTS-3APE film with 40.91 ± 10.18 MPa. Previous research has documented similar enhancements in tensile strength with increasing extract concentration [22]. Notably, the CTS-2APE film also showed an improvement in elongation at break, with the highest percentage of 119.00 ± 21.79%, indicating remarkable ductility. Thus, the CTS-2APE film, with the highest values in both tensile strength and elongation at break, emerges as the most optimized material among the films investigated.

Table 1. Thickness and mechanical behaviors of the synthesized films

Sample	Thickness (mm)	Tensile strength (MPa)	Elongation at break (%)
CTS	0.043 ± 0.013	39.63 ± 7.39	96.34 ± 27.75
CTS–1APE	0.043 ± 0.006	37.45 ± 17.08	93.74 ± 24.71
CTS–2APE	0.040 ± 0.000	51.72 ± 12.77	119.00 ± 21.79
CTS–3APE	0.040 ± 0.000	40.91 ± 10.18	95.88 ± 19.97

Moisture content, swelling degree, and solubility

To elucidate the impact of incorporating APE on certain properties of CTS-based films, pivotal parameters including moisture content, swelling degree, and solubility were investigated. Specifically, with the goal of applying the synthesized films as wound dressings, they need to absorb wound drainage and provide moisture to enhance re-epithelialization [23]. Wound drainage, also called exudate, consists of water, proteins, white blood cells, inflammatory components, and electrolytes, and plays a key role in wound healing [24]. However, excessive amounts or improper localization of wound drainage can delay the healing process. The achieved results are outlined in Table 2.

Moisture content refers to the total void volume occupied by water molecules within the microstructure network of films [25]. A decreasing trend in the moisture content of the synthesized films was observed with the increasing amount of incorporated extract. While the moisture content of the film fabricated with only CTS was recorded at 17.74 ± 0.50%, a noticeable drop to 14.84 ± 0.17% was seen for the CTS-1APE film. Similarly, the moisture content continued to fall to 14.10 ± 0.52% for the CTS-2APE film and 13.22 ± 0.56% for the CTS-3APE film. Hence, it can be concluded that the CTS-1APE film provides the highest moisture level among the CTS films blended with the extract. This phenomenon can be explained by the interaction between CTS and APE. This interaction decreases the accessibility of hydroxyl and amino groups, which are identified as hydrophilic functional groups. As a result, it limits CTS from interacting with water molecules through hydrogen bonding [26]. In contrast, as the amount of the extract blended increases, the solubility of the surveyed films after being immersed in a pH 7 solution for 24 hours gradually rises. The smallest solubility percentage, recorded at 17.78 ± 0.94%, belongs to the CTS film. With the addition of APE, the percentage of water solubility of the CTS-based films progressively increases, reaching its highest value of 25.13 ± 1.86% for CTS-3APE. Furthermore, the solubility percentages for CTS-1APE and CTS-2APE films were noted as 20.13 ± 0.88% and 22.19 ± 1.79%, respectively. The enhancement in solubility with the addition and increase in the blended amount of natural extracts such as rosemary, ginger, and sage into CTS-based films has also been documented in previous studies [27]. The swelling degree is a factor indicating the level of cross-linkage formed within a polymer network, which influences the water resistance of films. In simpler terms, the lower the degree of swelling, the greater the water-resistant ability of polymeric films. Additionally, the extent of swelling in a polymeric structure is heavily influenced by the quantity and nature of intermolecular chain interactions [19]. As shown in the table data, the swelling degree of the examined films also declines with increasing concentration of APE. The highest percentage of swelling degree was recorded for the CTS film at 55.51 ± 1.61%. Following the CTS film, the CTS-1APE and CTS-2APE had values of 45.88 ± 0.88% and 42.37 ± 1.39%, respectively. The film incorporated with the highest amount of extract, CTS-3APE, was reported to have the lowest value of 36.26 ± 1.93%. The hydrophobic interaction between polyphenols in the extract and the hydrophobic regions in the CTS matrix is responsible for the reduction in the degree of swelling [16].

Table 2. Moisture content, swelling degree, and solubility of synthesized films

Sample	Moisture content (%)	Swelling degree (%)	Solubility (%)
CTS	17.74 ± 0.50	55.51 ± 1.61	17.78 ± 0.94
CTS–1APE	14.84 ± 0.17	45.88 ± 0.88	20.13 ± 0.88
CTS–2APE	14.10 ± 0.52	42.37 ± 1.39	22.19 ± 1.79
CTS–3APE	13.22 ± 0.56	36.26 ± 1.93	25.13 ± 1.86

Characteristics of the films

The FTIR analysis was conducted to examine the possible functional groups in the synthesized films and their physical interactions. The FTIR spectra of the four fabricated films and the APE are shown in Figure 2. A wide absorption band at 3,200-3,420 cm^{-1} indicates a relative overlap between the –OH and N–H stretching vibrations. The –OH stretching is also detected at 3,845 cm^{-1} in the film. Additionally, the absorption peaks at 2,921 and 2,875 cm^{-1}, clearly depicted in the spectrum of CTS-1APE, are assigned to the C–H stretching vibrations of $–CH_3$ and $–CH_2$ groups [28]. The signal recorded from 1,630 to 1,645 cm^{-1} can be assigned to C=O stretching of amide groups, influenced by the degree of deacetylation of CTS. However, the prominent peak at 1,632 cm^{-1}, corresponding to the C=O stretching vibration in the sample containing only the extract, confirms the presence of the ester linkage from specific compounds within the extract. Additionally, the signal peaks at 1408, 1,405, and 1,403 cm^{-1} can be related to the aromatic C=C stretching vibration, while the existence of C–O stretching is validated by the corresponding absorption signals at 1,045, 1,024, and 1,025 cm^{-1}.

The SEM analysis was performed to investigate the surface morphology of the fabricated films. As shown in Figure 3, none of the four samples exhibited significant cracks, bulges, or abnormal pores on their surfaces. The SEM image of the film containing only CTS showed a relatively smooth surface with no fractures, aside from a white particle in the center of the image. This white particle in the CTS micrograph is likely a random aggregation of CTS molecules that have not fully dissolved [29]. Furthermore, small white spots appeared in all films when the extract was incorporated into the CTS matrix. Notably, as the concentration of the extract increased, the density of these small white spots also increased. The CTS-3APE film, which contains the highest amount of APE, exhibited a pronounced presence of these white spots. These spots are likely due to the insolubility of certain extract droplets. Similar features have been reported in previous studies [30].

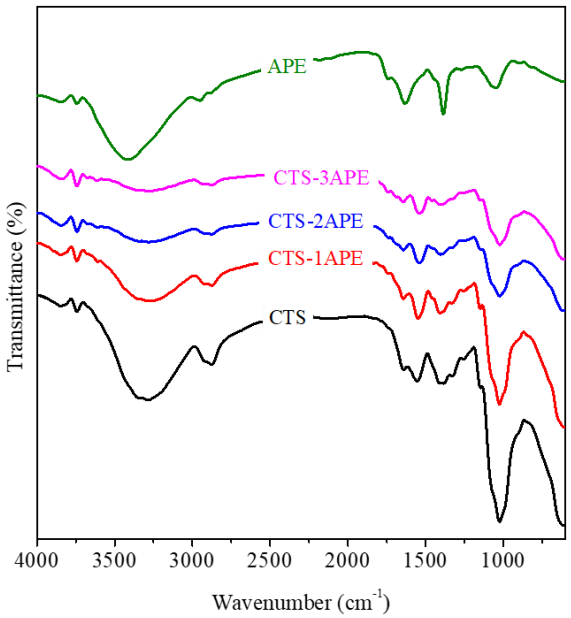

Figure 2. FTIR spectra of the synthesized films

The EDX analysis was performed to determine the presence and percentage of major elements in the fabricated films. Table 3 and Figure 4 present the elemental composition as mass percentages and EDX spectra of the analyzed films, respectively. The analysis confirmed the presence of three major elements: carbon, nitrogen, and oxygen, evidenced by peaks in the EDX spectra and their corresponding mass percentages. Carbon and oxygen account for over 90% of the

mass, with strong intensities observed at their respective energy levels, indicating their significant presence in all samples. Additionally, increases in the mass percentages of carbon and oxygen were noted as the amount of APE was increased. The analysis also confirmed the absence of any anomalous elements in the synthesized films, ensuring their integrity and suitability for further analysis and applications.

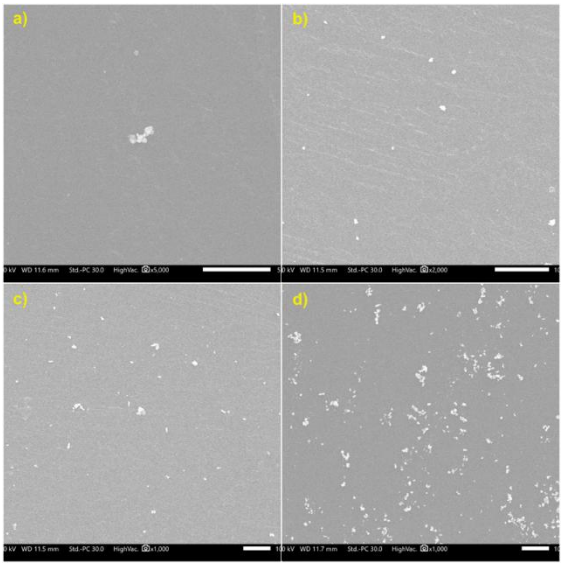

Figure 3. SEM images of (a) CTS and (b-d) CTS–xAPE

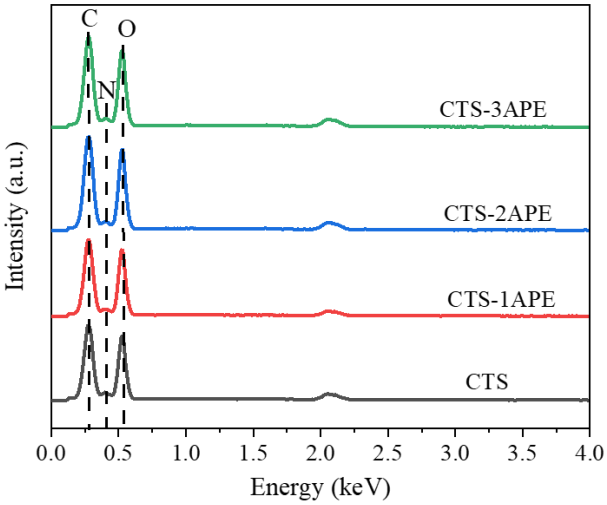

Figure 4. EDX spectra of the synthesized films

Table 3. Elemental composition of the synthesized films

Elements	Mass (%)			
	CTS	CTS–1APE	CTS–2APE	CTS–3APE
C	47.88 ± 0.12	48.27 ± 0.12	48.65 ± 0.11	48.40 ± 0.11
N	4.98 ± 0.12	4.08 ± 0.11	4.07 ± 0.10	4.21 ± 0.11
O	47.14 ± 0.25	47.66 ± 0.25	47.27 ± 0.22	47.39 ± 0.23
Total	100.00	100.00	100.00	100.00

Antibacterial activity

Antibacterial activity is a fundamental prerequisite for promoting wound healing processes [31]. In this study, the antibacterial properties of the films were evaluated using the Kirby-Bauer well diffusion method, with gentamicin serving as the positive control (very strong inhibition). *S. aureus* and *P. aeruginosa* were chosen as indicator bacteria due to their roles as common pathogens responsible for various infections and clinical diseases in humans [32]. The assay results confirmed the antibacterial activity of the films against both *S. aureus* and *P. aeruginosa* (Figure 5). Table 4 presents the inhibition zone diameters for the extract and synthesized films against both Gram-positive and Gram-negative bacterial strains.

Notably, the solutions of CTS-3APE and CTS-2APE films demonstrated the high antibacterial activity when compared to CTS-1APE, exhibiting a significantly larger inhibition zone compared to the negative control, which showed no inhibition, and CTS films, which served as the baseline with weaker antibacterial activity. The inherent antibacterial properties of CTS against both Gram-positive and Gram-negative bacteria [33] likely contributed to the observed differences.

Table 4. Zone of inhibition diameter

Samples	Zone of inhibition	
	S. aureus	***P. aeruginosa***
Negative control	No inhibition	No inhibition
Positive control (Gentamicin)	Very strong	Very strong
CTS	Weak	Weak
CTS–1APE	Medium	Medium
CTS–2APE	Strong	Strong
CTS–3APE	Strong	Strong

Notes: The descriptions represent the size of the inhibition zones as follows: (No inhibition) indicates no inhibition zone (0 mm), (Weak) represents an inhibition zone smaller than 3 mm, (Medium) corresponds to an inhibition zone smaller than 6 mm, (Strong) denotes an inhibition zone smaller than 9 mm, and (Very strong) signifies an inhibition zone larger than 15 mm.

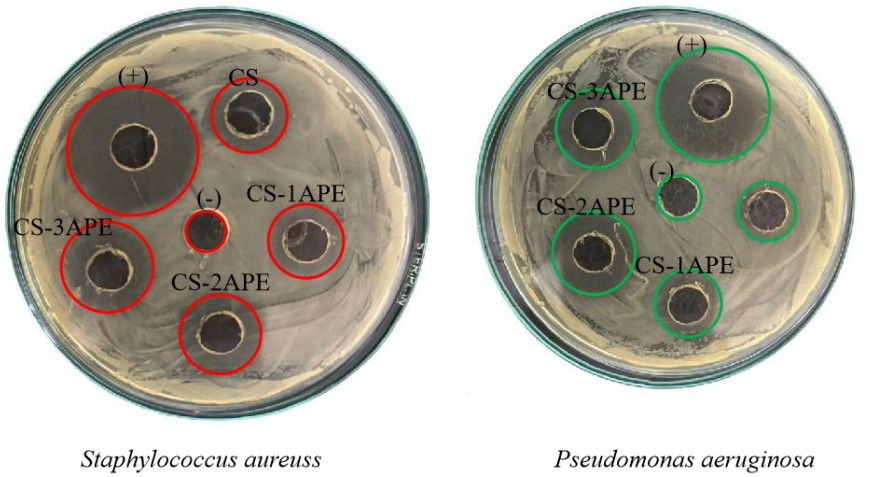

Figure 5. Zones of inhibition against *S. aureus* and *P. aeruginosa*

Interestingly, the bacteriostatic effect against both strains generally increased with higher concentrations of the extract at 2%.

The enhanced antibacterial performance of the films containing the extract can be attributed to bioactive compounds present in *A. paniculata*, such as andrographolide and phenolic compounds. These compounds likely synergize with the properties of CTS to improve the films' effectiveness against microbial strains.

Anti-inflammatory properties

The *in vitro* anti-inflammatory properties of the synthesized films and extract were evaluated using the egg albumin denaturation assay. The anti-inflammatory properties of the examined samples are illustrated in Figure 6. The results clearly show that CTS alone exhibits negligible anti-inflammatory activity across all concentrations, with nearly 0% inhibition of protein denaturation. In contrast, the films blended with the extract (CTS-xAPE) demonstrated significant inhibition of protein denaturation at all concentrations tested. The percentage of inhibition for these films increased with higher concentrations of the extract. While the anti-inflammatory activity of CTS films blended with the extract was evident across various concentrations, the effect of APE alone was only noticeable at lower concentrations. Overall, incorporating the extract into CTS films significantly enhances their anti-inflammatory activity, making them suitable for use in wound dressings.

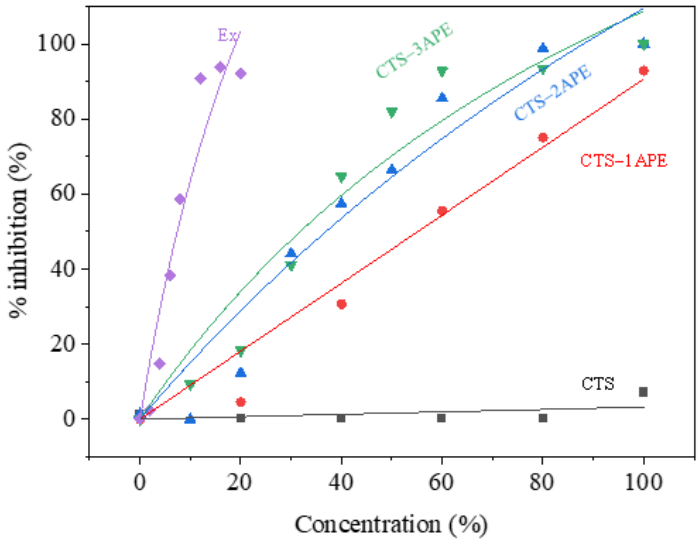

Figure 6. Anti-inflammatory performance of synthesized films and extract

Conclusion

In this study, CTS films incorporated with APE at varying volumes (1–3 mL) were successfully synthesized using the supercritical CO_2 extraction method, a green and sustainable technique. The CTS film blended with 3 mL of APE (CTS-3APE) demonstrated exceptional UV-blocking capabilities, achieving 0% transmittance in the UV-C and UV-B ranges and a maximum of 10% transmittance in the UV-A range. Despite the incorporation of APE, only negligible effects on film thickness were observed, while significant improvements were noted in tensile strength, elongation at break, swelling degree, moisture content, and solubility. Regarding mechanical properties, the CTS-3APE film exhibited excellent mechanical resistance and flexibility. Additionally, it showed significantly enhanced antibacterial activity compared to CTS alone. The presence of the extract also markedly improved the film's anti-inflammatory activity across various concentrations. These findings highlight the potential of CTS films incorporated with APE for a wide range of biomedical applications, particularly in wound healing, due to their superior mechanical properties, UV protection, antibacterial efficacy, and anti-inflammatory capabilities.

Disclosure Statement

No potential conflict of interest was reported by the authors in this work.

ORCID

Le Ngoc Quynh Chau:
https://orcid.org/0009-0000-3324-7438
Pham Trong Liem Chau:
https://orcid.org/0000-0001-8717-1416
Tran Nguyen Cam Nhung:
https://orcid.org/0009-0004-4071-5251
Huynh Ngoc Oanh:
https://orcid.org/0009-0007-3294-7679
Le Xuan Tien:
https://orcid.org/0000-0003-2762-8925
Nguyen Huu Hieu
https://orcid.org/0000-0003-1776-9871

References

[1] Mulla, M.Z., Ahmed, J., Vahora, A., Pathania, S. Effect of pectin incorporation on characteristics of chitosan based edible films. *Journal of Food Measurement and Characterization*, **2023**, 17(6), 5569-5581.

[2] Zhao, J., Wang, Y., Li, J., Lei, H., Zhen, X., Gou, D., Liu, T. Preparation of chitosan/Enoki mushroom foot polysaccharide composite cling film and its application in blueberry preservation. *International Journal of Biological Macromolecules*, **2023**, 246, 125567.

[3] Malik, Z., Parveen, R., Parveen, B., Zahiruddin, S., Khan, M.A., Khan, A., Husain, S.A. Anticancer potential of andrographolide from Andrographis paniculata (Burm. f.) Nees and its mechanisms of action. *Journal of Ethnopharmacology*, **2021**, 272, 113936.

[4] Dey, S., Veerendra, G., Babu, P.A., Manoj, A.P., Nagarjuna, K. Degradation of plastics waste and its effects on biological ecosystems: A scientific analysis and comprehensive review. *Biomedical Materials & Devices*, **2024**, 2(1), 70-112.

[5] Yuan, G., Lv, H., Yang, B., Chen, X., Sun, H. Physical properties, antioxidant and antimicrobial activity of chitosan films containing carvacrol and pomegranate peel extract. *Molecules*, **2015**, 20(6), 11034-11045.

[6] Kaya, M., Khadem, S., Cakmak, Y.S., Mujtaba, M., Ilk, S., Akyuz, L., Deligöz, E. Antioxidative and antimicrobial edible chitosan films blended with stem, leaf and seed extracts of Pistacia terebinthus for active food packaging. *RSC Advances*, **2018**, 8(8), 3941-3950.

[7] Carrera, C., Bengoechea, C., Carrillo, F., Calero, N. Effect of deacetylation degree and molecular weight on surface properties of chitosan obtained from biowastes. *Food Hydrocolloids*, **2023**, 137, 108383.

[8] Pramanik, S., Aggarwal, A., Kadi, A., Alhomrani, M., Alamri, A.S., Alsanie, W.F., Bellucci, S. Chitosan alchemy: transforming tissue engineering and wound healing. *RSC Advances*, **2024**, 14(27), 19219-19256.

[9] Kalariya, K.A., Gajbhiye, N.A., Meena, R.P., Saran, P.L., Minipara, D., Macwan, S., Geetha, K. Assessing suitability of Andrographis paniculata genotypes for rain-fed conditions in semi-arid climates. *Information Processing in Agriculture*, **2021**, 8(2), 359-368.

[10] Shahbazi, Y. Characterization of nanocomposite films based on chitosan and carboxymethylcellulose containing Ziziphora clinopodioides essential oil and methanolic Ficus carica extract. *Journal of Food Processing and Preservation*, **2018**, 42(2), e13444.

[11] Chau, T.P., Samdani, M.S., Kuriakose, L.L., Sindhu, R. Assessment of multi-biomedical efficiency of Andrographis paniculata shoot extracts through in-vitro analysis and major compound identification. *Environmental Research*, **2024**, 242, 117779.

[12] Dinh, T.A., Le, Y.N., Pham, N.Q., Ton-That, P., Van-Xuan, T., Ho, T.G.T., Phuong, H.H.K. Fabrication of antimicrobial edible films from chitosan incorporated with guava leaf extract. *Progress in Organic Coatings*, **2023**, 183, 107772.

[13] Wang, D., Shao, S., Wang, B., Guo, D., Tan, L., Chen, Q. Fabrication of chitosan/guar gum/polyvinyl alcohol films incorporated with polymethoxyflavone-rich citrus extracts: Postharvest shelf-life extension of strawberry fruits. *Progress in Organic Coatings*, **2024**, 194, 108611.

[14] Tien, N.N.T., Nguyen, H.T., Le, N.L., Khoi, T.T., Richel, A. Biodegradable films from dragon fruit (Hylocereus polyrhizus) peel pectin and potato starches crosslinked with glutaraldehyde. *Food Packaging and Shelf Life*, **2023**, 37, 101084.

[15] Dkhil, M.A., Zreiq, R., Hafiz, T.A., Mubaraki, M.A., Sulaiman, S., Algahtani, F., Al-Quraishy, S. Anthelmintic and antimicrobial activity of Indigofera oblongifolia leaf extracts. *Saudi Journal of Biological Sciences*, **2020**, 27(2), 594-598.

[16] Rahman, L., Goswami, J., Choudhury, D. Assessment of physical and thermal behaviour of chitosan-based biocomposites reinforced with leaf and stem extract of Tectona grandis. *Polymers and Polymer Composites*, **2022**, 30, 09673911221076305.

[17] Due, E., Rossen, K., Sorensen, L.T., Kliem, A., Karlsmark, T., Haedersdal, M. Effect of UV irradiation on cutaneous cicatrices: A randomized, controlled trial with clinical, skin reflectance, histological, immunohistochemical and biochemical evaluations. *Acta Dermato-Venereologica*, **2007**, 87(1), 27-32.

[18] Özcan, G., Shenaq, S., Chahadeh, H., Spira, M. Ultraviolet-A induced delayed wound contraction and decreased collagen content in healing wounds and implant capsules. *Plastic and Reconstructive Surgery*, **1993**, 92(3), 480-484.

[19] Nguyen, T.T., Dao, U.T.T., Bui, Q.P.T., Bach, G.L., Thuc, C.H., Thuc, H.H. Enhanced antimicrobial activities and physiochemical properties of edible film based on chitosan incorporated with Sonneratia caseolaris (L.) Engl. leaf extract. *Progress in Organic Coatings*, **2020**, 140, 105487.

[20] Kalaycıoğlu, Z., Torlak, E., Akın-Evingür, G., Özen, İ., Erim, F.B. Antimicrobial and physical properties of chitosan films incorporated with turmeric extract. *International Journal of Biological Macromolecules*, **2017**, 101, 882-888.

[21] Sánchez-González, L., Vargas, M., González-Martínez, C., Chiralt, A., Cháfer, M. Characterization of edible films based on hydroxypropylmethylcellulose and tea tree essential oil. *Food Hydrocolloids*, **2009**, 23(8), 2102-2109.

[22] Siripatrawan, U., Vitchayakitti, W. Improving functional properties of chitosan films as active

food packaging by incorporating with propolis. *Food Hydrocolloids*, **2016**, 61, 695-702.
[23] Obagi, Z.; Damiani, G.; Grada, A.; Falanga, V. Principles of wound dressings: A review. *Surgical Technology International*, **2019**, 35(5), 50-57.
[24] Cutting, K.F. Wound exudate: composition and functions. *British Journal of Community Nursing*, **2003**, 8(Sup3), S4-S9.
[25] Pereda, M., Ponce, A., Marcovich, N., Ruseckaite, R., Martucci, J. Chitosan-gelatin composites and bi-layer films with potential antimicrobial activity. *Food Hydrocolloids*, **2011**, 25(5), 1372-1381.
[26] Ojagh, S.M., Rezaei, M., Razavi, S.H., Hosseini, S.M.H. Development and evaluation of a novel biodegradable film made from chitosan and cinnamon essential oil with low affinity toward water. *Food Chemistry*, **2010**, 122(1), 161-166.
[27] Souza, V.G.L., Fernando, A.L., Pires, J.R.A., Rodrigues, P.F., Lopes, A.A., Fernandes, F.M.B. Physical properties of chitosan films incorporated with natural antioxidants. *Industrial Crops and Products*, **2017**, 107, 565-572.
[28] Aleem, A.R., Shahzadi, L., Tehseen, S., Alvi, F., Chaudhry, A.A., ur Rehman, I., Yar, M. Amino acids loaded chitosan/collagen based new membranes stimulate angiogenesis in chorioallantoic membrane assay. *International Journal of Biological Macromolecules*, **2019**, 140, 401-406.
[29] Rihayat, T., Hadi, A.E., Aidy, N., Safitri, A., Siregar, J.P., Cionita, T., Fitriyana, D.F. Biodegradation of polylactic acid-based bio composites reinforced with chitosan and essential oils as anti-microbial material for food packaging. *Polymers*, **2021**, 13(22), 4019.
[30] Yong, H., Wang, X., Bai, R., Miao, Z., Zhang, X., Liu, J. Development of antioxidant and intelligent pH-sensing packaging films by incorporating purple-fleshed sweet potato extract into chitosan matrix. *Food Hydrocolloids*, **2019**, 90, 216-224.
[31] Liang, Y., He, J., Guo, B. Functional hydrogels as wound dressing to enhance wound healing. *ACS Nano*, **2021**, 15(8), 12687-12722.
[32] Pagliarulo, C., De Vito, V., Picariello, G., Colicchio, R., Pastore, G., Salvatore, P., Volpe, M.G. Inhibitory effect of pomegranate (*Punica granatum* L.) polyphenol extracts on the bacterial growth and survival of clinical isolates of pathogenic Staphylococcus aureus and Escherichia coli. *Food Chemistry*, **2016**, 190, 824-831.
[33] Li, J., Zhuang, S. Antibacterial activity of chitosan and its derivatives and their interaction mechanism with bacteria: Current state and perspectives. *European Polymer Journal*, **2020**, 138, 109984.

HOW TO CITE THIS ARTICLE

L.N.Q. Chau, P.T.L. Chau, T.N.C. Nhung, H.N. Oanh, L. X. Tien, N.H. Hieu, Synthesis of Chitosan Films Incorporated with *Andrographis Paniculata* (Burm. F.) Nees Extract by Supercritical CO_2 Technique and Their Biological Activities. *Adv. J. Chem. A*, 2026, 9(7), 1363-1376.

DOI: 10.48309/AJCA.2026.572011.2035
URL: https://www.ajchem-a.com/article_241368.html